Available online at www.sciencedirect.com
ScienceDirect
Journal of Power Sources 178 (2008) 434–438
JOURNAL OF POWER SOURCES
www.elsevier.com/locate/jpowsour

Short communication

Characteristics of Sn/Li_2O multilayer composite anode for thin film microbattery

Jae Joon Lee [a], Soo Ho Kim [a], Seung Hyun Jee [a], Young Soo Yoon [a,*], Won Il Cho [b], Seok Jin Yoon [c], Ji Won Choi [c], Sang-Cheol Nam [d,*]

[a] *Department of Advanced Technology Fusion, Konkuk University, 1 Hwayang dong, Gwang jin, Seoul 143-701, Republic of Korea*
[b] *Battery and Fuel Cell Research Center, KIST, P.O. Box 131, Seoul 130-650, Republic of Korea*
[c] *Thin Film Research Center, KIST, P.O. Box 131, Seoul 130-650, Republic of Korea*
[d] *Nuricell Inc., GS Caltex New Energy Development Center, Seongnae 1-dong, Gangdong-gu, Seoul, Republic of Korea*

Received 9 August 2007; received in revised form 11 October 2007; accepted 29 November 2007
Available online 28 December 2007

Abstract

Sputtering growth of a Sn/Li_2O multilayer composite thin film is conducted to produce an anode thin film with less capacity fading than that of a pure SnO_2 film for a thin-film battery. The structural properties of the Sn/Li_2O multilayer are examined. In addition, the electrochemical characteristics of the Sn/Li_2O and pure SnO_2 thin films are compared. X-ray diffraction and transmission electron microscopy measurements reveal a Sn crystalline peak only and a $Sn–Li_2O$ multilayer structure, respectively, in the Sn/Li_2O thin film. A SnO_2 thin film with a polycrystalline phase shows an irreversible side-reaction at 0.8 V versus Li/Li^+, an initial charge retention of about 29%, and poor cycleability in the cut-off voltage range from 1.2 to 0 V versus Li/Li^+. By contrast, no irreversible side-reaction is found in the Sn/Li_2O multilayer composite thin film while there is an initial charge retention of 49% and better cycleability (more than twice) than that of pure SnO_2 film after about 150 cycles. These results indicate that the Sn/Li_2O multilayer composite thin film can be used for tin-based, thin-film, microbatteries and provide motivation to pursue fabrication of $Sn–Li_2O$ anode powder for bulk type batteries.

Keywords: Sn/Li_2O multilayer; Tin oxide; Thin-film anode; Tin-based battery; Cycleability; Charge retention

1. Introduction

Tin-based materials are promising alternative anode electrode materials for rechargeable lithium-ion batteries [1]. In particular, SnO_2 is a good candidate material for the anode of thin-film microbatteries since SnO_2 thin films can be synthesized by a simple process at a relatively low temperature below 300 °C. Low-pressure chemical vapour deposition (LPCVD) growth of crystalline SnO_2 films has been reported by Brousse et al. [2] with the films showing a high capacity that lasts for more than 100 cycles. However, SnO_2 suffers from poor electrochemical behaviour during the charge–discharge process due to its structural instability [3]. Studies of the doping of Si and/or Mo in SnO_2 for improvement in capacity and cycleability have been reported [4,5] whereas Yang et al. [6] obtained 360 mAh g^{-1} and 200 cycles for a polycrystalline Sn–SnSb composite with a particle size below 300 nm. Nevertheless, tin-based anode materials are not adequate for use as an anode in their original form due to the formation of an irreversible phase via a side-reaction, which induces an irreversibility of capacity of greater than approximately 70% near 0.8 V versus Li/Li^+ during the first charging state.

Tin-based anode materials have many advantages over carbon from a practical point of view and could feasibly be adopted for rechargeable batteries or thin-film microbatteries if the above-mentioned problems could be solved. Nevertheless, a tin-based thin film anode is not appropriate for application in thin-film

* Corresponding authors.
E-mail addresses: ysyoon@konkuk.ac.kr (Y.S. Yoon), scnam@nuricell.com (S.-C. Nam).

0378-7753/$ – see front matter © 2008 Elsevier B.V. All rights reserved.
doi:10.1016/j.jpowsour.2007.11.116

microbatteries even though the cycleability is better than that of bulk or powdered tin-based materials since a very large volume change occurs during the charge–discharge process. This induces microcracks in the thin film that results in rapid capacity decrease after roughly 120 cycles [7–9]. Courtney and Dahn [10,11] reported that Li atoms do not intercalate inside the SnO_2 crystal lattice when SnO_2 is employed as an anode. Meanwhile, there is formation of irreversible phases such as Li_2O and metallic Sn during the first charge, allowing a reversible alloying reaction process between Li and Sn during subsequent cycles, as indicated by *in situ* X-ray diffraction (XRD) observations.

Thus, it can be speculated that a Li_2O-metal Sn composite could be applied as an anode material. Notably, it would offer good cycleability, since sequential formation of Li_2O irreversible phases by the reaction between Li from the cathode and SnO_2 could be prevented during Li intercalation and de-intercalation. In this paper, we investigate the structural and electrochemical properties of a Sn/Li_2O multilayer composite thin film that offers: (i) reduced irreversibility caused by Li_2O formation and (ii) improved cycling performance. By using a co-sputtering system with two different targets, a Sn/Li_2O multilayer composite thin film and a SnO_2 thin film are deposited. The electrochemical behaviour of these thin films are compared.

2. Experimental

A sample of 4 in. SnO_2 with a purity of 99.99% and Ar gas with a purity of 99.999% as a sputter target and a sputtering gas, respectively. 304 stainless-steel current-collector thin film coated soda lime glass substrates were decreased three times in warm acetone and trichloroethylene (TCE) and then rinsed thoroughly with de-ionized water with a resistivity of above several $10^8\ \Omega$ cm. After the substrates were evacuated to 5×10^{-6} Torr, deposition was carried out at 300 °C. Prior to SnO_2 growth, the SnO_2 target was cleaned to remove surface contaminations by means of Ar^+ sputtering ions. Deposition of SnO_2 thin films was carried out via horizontal on-axis type sputtering with a radio frequency (RF) power of 100 W. The substrate was rotated at 10 rpm in order to improve the film homogeneity during the film growth. Cross-sectional scanning electron microscopy (SEM) and α-step were employed to confirm the thickness of the SnO_2 films (300 nm). The working pressure was 8 m Torr under an Ar gas flow rate of 14 sccm. Structural and electrochemical measurements were conducted on SnO_2 thin films with a deposition area of 1.5 cm × 1.5 cm.

Sn–Li_2O multilayer thin films with four Sn metal layers and three Li_2O layers were deposited by a direct current (dc) and RF sputtering system, respectively, on substrates that were prepared by the same process used for deposition of the SnO_2 film. The Li_2O target is a very hygroscopic material and must be treated in a dry room with a dew point of 69.5 °C. The thickness of single Sn and Li_2O layers was 70 and 60 nm, respectively. The dc and RF power for the Sn and Li_2O were 2.3 and 100 W, respectively. The base pressure, working pressure, gas flow rate, and deposition area were those used for the SnO_2 thin film.

After capacitance measurements, the capacities of both anode thin films were calculated using an average density value of Li_2O (2 g cm^{-3}) and Sn (7.3 g cm^{-3}). Surface and cross-section views of the films were obtained via SEM and transmission electron microscopy (TEM). The crystalline properties of the films were examined by a wide-angle XRD analysis.

Half-cell tests were carried out to compare the electrochemical behaviour. Half-cells were assembled with lithium foils (Cyprus) as the counter and reference electrodes and 1 M $LiPF_6$ in EC:DMC (1:1, Merck) as the electrolyte solution. A polyethylene-based separator (Ube) was used. Cell assembly was conducted in a dryroom below the dew point, i.e., 65.5 °C. Constant-current galvanostatic charge–discharge measurements were performed to investigate capacity and cycling properties.

3. Results and discussion

The SnO_2 and Sn/Li_2O multilayer thin films have a mirror-like surface without any indication of defects such as cracks, groves, pinholes or pores, as confirmed by visible inspection and Normarski optical microscopy. Fig. 1 shows the XRD patterns of: (a) SnO_2 and (b) Sn/Li_2O multilayer thin films. Based on the JCPD41-1445, the as-deposited pure SnO_2 thin film has (1 1 0), (1 0 1), (2 0 0) and (2 1 1) crystalline peaks, as shown in (a). Metallic Sn(2 0 0), (1 0 1) and (2 1 1) peaks are detected in (b) as well as a current-collect peak, S, but no Li_2O peaks are observed, which indicates a lack of long-range order of Li_2O in the Sn/Li_2O multilayer. In summary, the XRD pattern for the Sn/Li_2O layer reveals a multilayer structure with a crystalline Sn layer and an amorphous Li_2O layer.

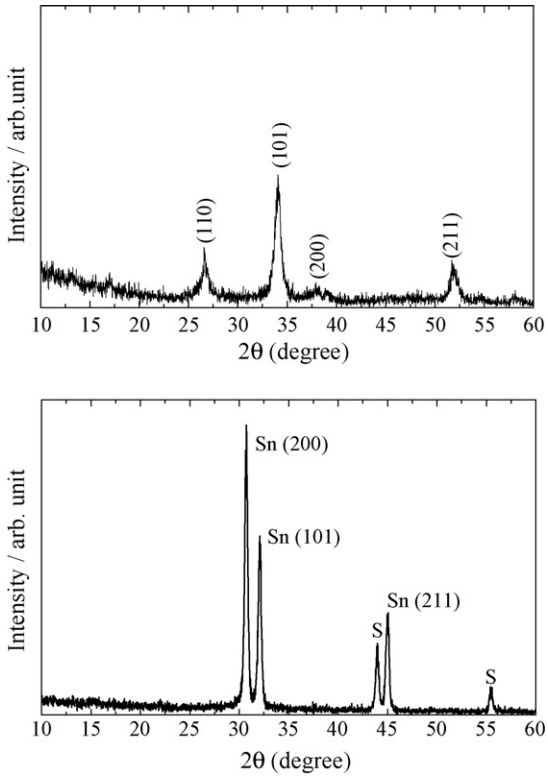

Fig. 1. XRD patterns of: (a) pure SnO_2 thin film deposited at 300 °C and (b) Sn/Li_2O multilayer thin film.

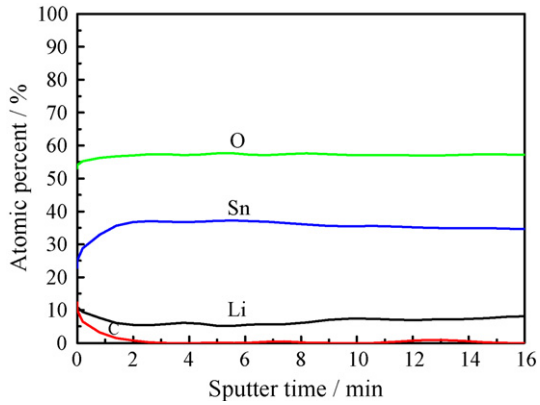

Fig. 2. Auger depth profile for Sn/Li_2O multilayer thin film.

To confirm the presence of elements according to each layer or region, Auger electron spectroscopy (AES) investigation of the depth profile analysis was undertaken, as illustrated in Fig. 2. The results show that the Sn/Li_2O multilayer thin film consists of lithium, tin and oxygen atoms. The AES depth profile indicates that the lithium, tin and oxygen atoms are very uniformly distributed under the surface layer after 16 min sputtering from the surface despite the fact that the deposited thin film was thought to have a Sn/Li_2O multilayer structure. Therefore, it is necessary to investigate the interface structure by means of electron microscopy such as SEM or TEM.

The Sn/Li_2O multilayer thin film has a fairly smooth surface without any voids and/or cracks. The SEM micrograph reveals that the surface layer has crystal-like characteristics, such as the presence of grain and grain boundaries, as shown in Fig. 3(a). The morphology is reflective of a typical surface structure of a crystalline thin film. This can be attributed to the Sn layer deposition as a surface end-layer of the Sn/Li_2O multilayer structure. Even though Sn/Li_2O multilayer thin films are deposited, the cross-sectional SEM image (Fig. 3(b)) does not reveal any interface between the Sn and the Li_2O layers. To examine the interface structure, a cross-sectional TEM (XTEM) examination was performed.

A high resolution XTEM image obtained from the Sn/Li_2O multilayer thin film is presented in Fig. 4(a). The image reveals an interface feature between Sn and Li_2O that is consistent with the experimental procedure. It should be noted that in addition to dark blobs, a white region is present. The TED pattern obtained from the Sn/Li_2O multilayer thin film exhibits an extra diffusion ring that has many small diffracted spots, which is indicative of the presence of both amorphous and crystalline phases, as shown in Fig. 4(b). This diffraction feature suggests that the Sn/Li_2O multilayer thin film has both crystalline and amorphous phases, which agrees well with the XRD results shown in Fig. 1. The XRD, TEM images and TED results reveal that the Sn/Li_2O multilayer thin film consists of amorphous Li_2O and crystalline Sn. The regions with dark blobs and the white regions are thought to be crystalline Sn and amorphous Li_2O, respectively. This finding agrees well with the XRD result.

The cycling features of the pure SnO_2 and the Sn/Li_2O multilayer thin films in a cut-off voltage range from 1.2 to 0 V

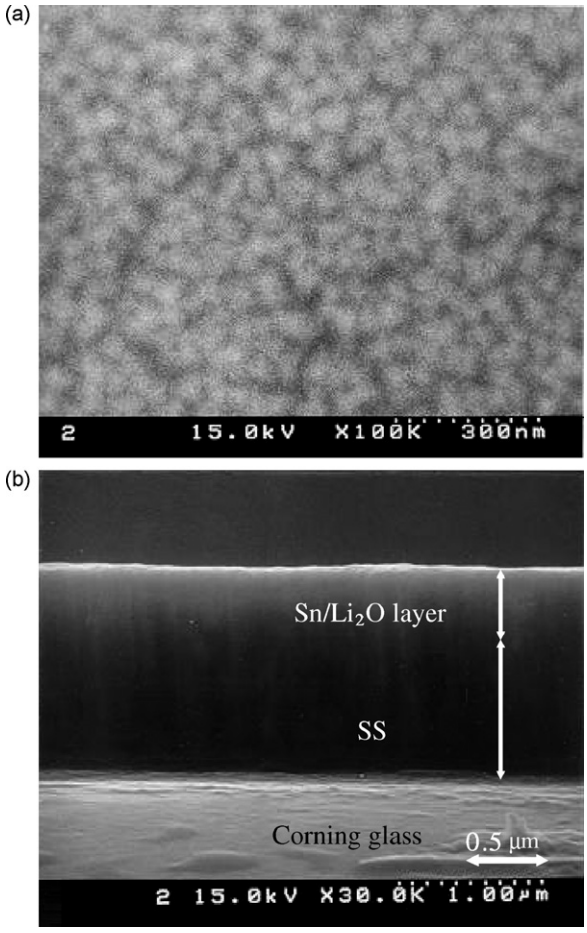

Fig. 3. SEM images of: (a) surface and (b) cross-section of Sn/Li_2O multilayer thin film.

versus Li/Li^+ at a constant current of 1.96 mA are presented in Fig. 5. Comparing the capacity of the first and second cycling stages of both films, the capacity retention of the pure SnO_2 and the Sn/Li_2O multilayer thin film are 29 and 49%, respectively. The small retention value of the SnO_2 film originates from the formation of amorphous lithium oxide, which occurs in a discharge voltage range of 0.7–0.9 V versus Li/Li^+ and metallic Sn at the first stage. By contrast, the Sn/Li_2O multilayer thin film gives a charge capacity retention of around 50%, which suggests that there is no irreversible side-reaction in the discharge voltage range of 0.7–0.9 V versus Li/Li^+ at the first stage. The Sn/Li_2O multilayer thin film displays better cycling characteristics, while the pure SnO_2 shows rapid capacity degradation below approximately 150 cycles, which is caused by the formation of many cracks on the surface of the pure SnO_2 thin film, as shown in Fig. 6. The inner impedance is expected to increase when Li_2O is inserted between the metallic Sn layers since the Li_2O does not contribute to any intercalation reaction and is an extremely poor ionic conductor for lithium transfer. Therefore, the inner impedance of the Sn/Li_2O multilayer thin film is expected to be higher than that of the SnO_2 film. In general, low inner impedance equates to better performance. Nevertheless, better cycleability is found in the Sn/Li_2O multilayer thin film.

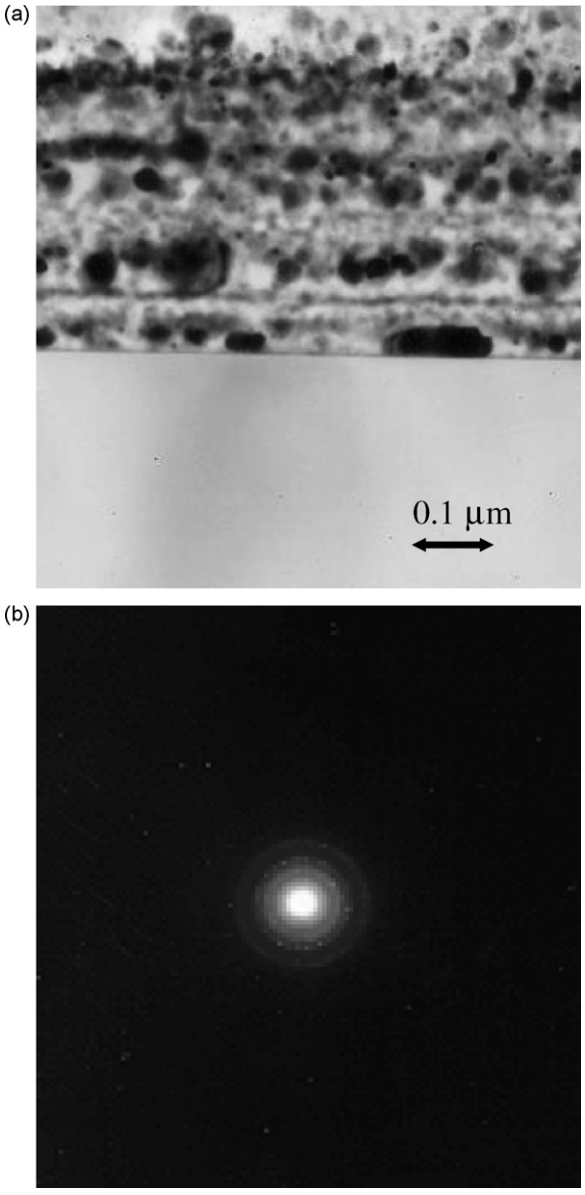

Fig. 4. (a) Cross-sectional TEM image and (b) TED pattern of Sn/Li_2O multilayer thin film.

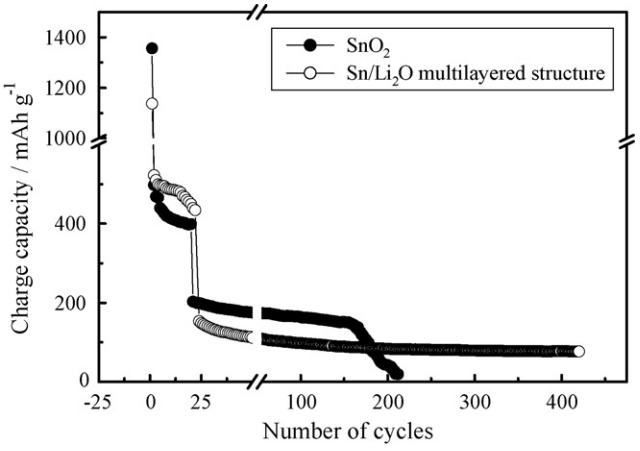

Fig. 5. Cycling characteristics of pure SnO_2 and Sn/Li_2O multilayer thin films.

An analysis of the surface SEM images was carried out to examine this phenomenon. Fig. 6 shows the surface structures of pure SnO_2 and Sn/Li_2O multilayer thin films after 160 and 500 cycles, respectively. The surface of the pure SnO_2 has serious defects such as cracks and holes. Since both films have very smooth surfaces without cracks, it can be concluded that the defects are formed during the charge–discharge process. That is, the cycling process induces a volume expansion of SnO_2, which causes stresses or strains. The strains result in the formation of microcracks and finally surface cracking. However, the defects on the surface of the Sn/Li_2O multilayer thin film are not serious compared with those on pure SnO_2. Therefore, the formation of defects on the surface might be restricted by the introduction of Li_2O layers between the Sn layers. Even though it cannot be clearly explained at present, the mechanism by which the Li_2O layer prevents the formation of defects might involve strain absorption by the soft Li_2O layer. If the strains induced by volume expansion of the Sn metal layers are perpendicular to the Li_2O layer, the Li_2O layer can easily absorb a portion of the total strains. That is, the total amount of strain in the Sn/Li_2O multilayer thin film is much smaller than that in the pure SnO_2, which can reduce the formation of defects. Schematic diagrams of these mechanisms are presented in Fig. 7.

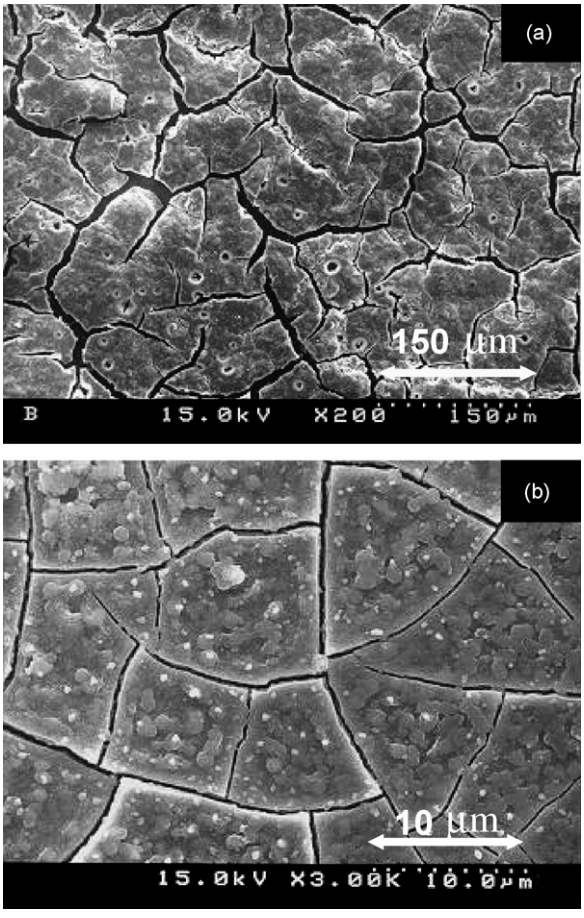

Fig. 6. SEM surface images of: (a) pure SnO_2 layer after 160 cycles and (b) Sn/Li_2O multilayer thin film after 500 cycles.

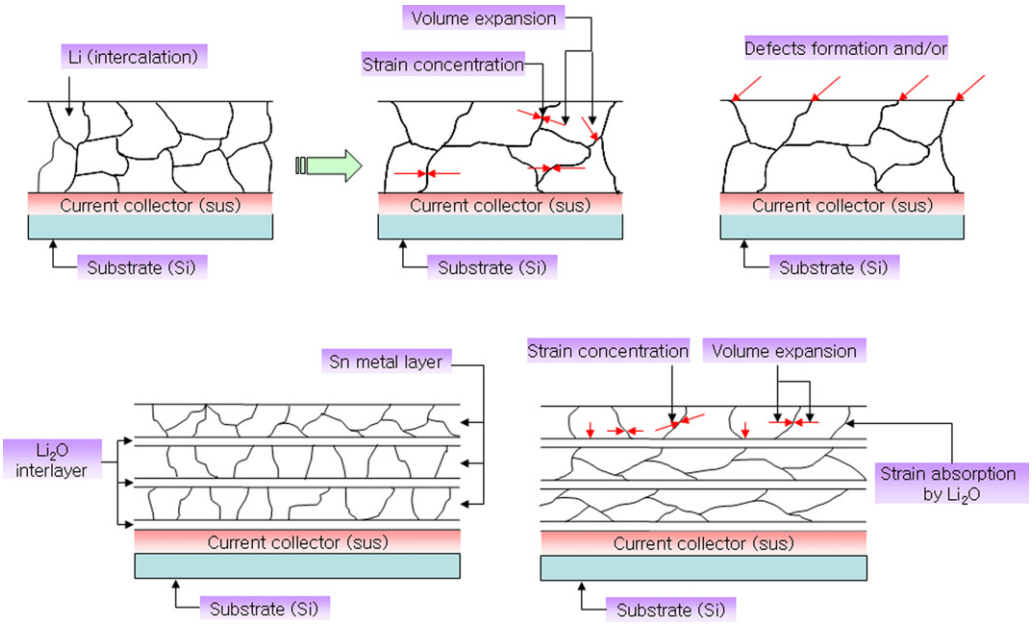

Fig. 7. Schematic diagrams of formation of defects and strain relaxation mechanism for: (a) pure SnO_2 and (b) Sn/Li_2O multilayer thin film, respectively.

4. Conclusions

The structural and electrochemical properties of a Sn/Li_2O multilayer thin film in terms of potential application as an anode for a secondary microbattery have been investigated using XRD, AES, SEM, TEM, TED, and a battery cycler. The Sn/Li_2O multilayer thin film exhibits better cycleability than a pure SnO_2 thin film. In particular, the Sn/Li_2O multilayer thin film shows remarkably improved retention at the initial charge–discharge stage. From cross-sectional TEM results, an interface feature between Sn and Li_2O is observed. While the precise mechanism for the improvement of the electrochemical properties is not clearly understood at present, it is thought that a strain absorption effect of the Li_2O layers between the Sn layers might be a critical factor. That is, the total amount of strain in the Sn/Li_2O multilayer thin film is much smaller than that in pure SnO_2 since the Li_2O layer can absorb the strains that are perpendicular to the Li_2O or Sn layers.

References

[1] Y. Idota, M. Mishima, M. Miyaki, T. Kubota, T. Miyasaka, Eur. Pat. Appl. 651450 Al 950503.
[2] T. Brousse, R. Retoux, U. Herterich, D.M. Schleich, J. Electrochem. Soc. 145 (1998) 1.
[3] S.C. Nam, Y.S. Yoon, W.I. Cho, B.W. Cho, H.S. Chun, K.S. Yun, J. Electrochem. Soc. 148 (1998) 220.
[4] H. Hung, E.M. Kelder, I. Chen, J. Schoonman, J. Power Sources 81 (1999) 362.
[5] J. Morales, L. Sanchez, J. Electrochem. Soc. 146 (1999) 1640.
[6] J. Yang, M. Wachtler, M. Winter, J.O. Besenhard, Electrochem. Solid-State Lett. 2 (1999) 161.
[7] S.C. Nam, Y.H. Kim, W.I. Cho, B.W. Cho, H.S. Chun, K.S. Yun, Electrochem. Solid-State Lett. 2 (1999) 9.
[8] S.C. Nam, C.H. Paik, W.I. Cho, B.W. Cho, H.S. Chun, K.S. Yun, J. Power Sources 84 (1999) 24.
[9] S.C. Nam, Y.S. Yoon, W.I. Cho, B.W. Cho, H.S. Chun, K.S. Yun, Electrochemistry 68 (2000) 32.
[10] I.A. Courtney, J.R. Dahn, J. Electrochem. Soc. 144 (2000) 2045.
[11] I.A. Courtney, J.R. Dahn, J. Electrochem. Soc. 144 (1997) 2943.